

MODEL OF A KUIPER BELT SMALL GRAIN POPULATION AND RESULTING FAR-INFRARED EMISSION

D. E. BACKMAN AND A. DASGUPTA

Department of Physics and Astronomy, Franklin and Marshall College, P.O. Box 3003, Lancaster, PA 17604;
d_backman@acad.fandm.edu; a_dasgupta@acad.fandm.edu

AND

R. E. STENCEL

Department of Physics and Astronomy, University of Denver, 2112 East Wesley Avenue, Denver, CO 80208; rstencil@phoenix.phys.du.edu

Received 1995 May 18; accepted 1995 June 22

ABSTRACT

We have calculated a simple model of the expected Kuiper Belt (KB) small grain population and the thermal emission that would arise from such grains. We have also sought observational evidence for this emission. The model assumed equilibrium between grain creation by collisional fragmentation of comets and removal by Poynting-Robertson radiation drag, radiation pressure-driven ejection, mutual collisions, and sublimation. The model far-IR intensity scales as the square of total KB mass.

Comparison of our model with observations of the zodiacal dust rules out emission from trans-Neptunian dust representing more than about $0.3 M_{\oplus}$ of KB comets. This agrees with recent *HST* reports of a population of comet-sized bodies in the KB which has a minimum mass of about $0.04 M_{\oplus}$, although that population can be extrapolated to include as much as $1 M_{\oplus}$ in the volume of our model. The model KB dust fractional bolometric luminosity ($L_{\text{dust}}/L_{\text{star}}$) would have about 10^{-2} and 10^{-4} of the values for the grain disks around Vega and β Pic, respectively.

A preliminary search in *COBE* DIRBE data reveals nonuniform bands near the ecliptic of cold ($T = 20\text{--}30$ K) emission prominent at wavelengths of 140 and 240 μm but not prominent relative to zodiacal emission at shorter (*IRAS*) wavelengths. Most of this emission is probably not from solar system material.

Subject headings: circumstellar matter — comets: general — planetary systems — solar system: general

1. INTRODUCTION

The Kuiper Belt (KB) is a zone of comets in the ecliptic plane beyond the orbit of Neptune, remnants of the solar system's formation (see reviews by Jewitt & Luu 1995; Weissman 1995). More than 20 large (100–300 km) objects have been found so far at heliocentric radii of 30–45 AU that could be members of the source dynamical population for short-period comets. Recently, a new population of bodies with diameters of a few times 10 km and orbit semimajor axes of ~ 40 AU have been reported in deep *HST* images (Cochran et al. 1995).

The “Vega/ β Pic” main-sequence disks may offer the best extrasolar analog to the KB (see review by Backman & Paresce 1993; Weissman 1995). These are systems of solid grains with temperatures of 50–150 K, fractional bolometric luminosities ($L_{\text{grains}}/L_{\text{star}}$) in the range 10^{-5} to 10^{-3} , and spatial scales similar to the KB. Common occurrence of these systems indicates reservoirs of large undetected parent bodies which resupply grains over system ages in some cases >1 Gyr against rapid removal processes. Weissman (1984) and Harper, Loewenstein, & Davidson (1984) suggested that the emission around Vega (α Lyr) is from grains liberated by sublimation or collisions in a cloud of comet-like bodies similar to the “Inner Oort Cloud” or KB.

Are the dust disks observed around many nearby main-sequence stars actually their “Kuiper Belts”? If our solar system were examined with an *IRAS*- or *ISO*-like instrument from the distance of β Pic, the only likely detectable component would be a hypothetical small grain population in the KB (Backman & Paresce 1993). Aumann & Good (1990) argue

that it would be peculiar if the Sun did not have at least a small amount of cold far-IR-emitting material because it appears that typical G main-sequence stars do in *IRAS* data. However, such material in the ecliptic outside the planetary zone could be difficult to detect from our position because of powerful interference from foreground zodiacal dust. If our solar system has a grain disk resembling the numerous Vega/ β Pic systems, then such a disk can be consistent with the presence of planets. This Letter includes a theoretical and observational investigation of the grain population beyond the planetary zone of the solar system and a comparison with general properties of prototypical main-sequence circumstellar disks.

2. MODEL CONSTRUCTION AND RESULTS

The equilibrium KB grain population in a set of radial annuli was calculated from local creation, destruction, and transport rates. Grains were assumed to be produced by (1) shattering collisions between comets moving along orbits of moderate inclination and eccentricity and (2) subsequent collisions of the fragments. Grains were assumed to be destroyed by (1) Poynting-Robertson (PR) radiation drag inducing inward drift to the planetary zone, (2) radiation pressure-driven ejection for the smallest grains, (3) mutual collisions, and (4) sublimation. These mechanisms will be discussed in more detail below.

2.1. Model Assumptions

Collisions between comets were assumed to occur as the result of random deviations from circular, coplanar orbits. Inclinations and eccentricities were assumed to be sufficiently

large to ensure shattering collisions (see below). The fractional cross section of comets perpendicular to the KB midplane in a given radial annulus was defined as $\tau_{\perp}(r) = N(r_1, r_2) \pi a_c^2 / \pi(r_2^2 - r_1^2)$, where $N(r_1, r_2)$ is the number of comets between r_1 and r_2 and a_c is the radius of a comet. An average collision frequency per comet was calculated from $1/t_{\text{coll}} = 2^{3/2} \pi \tau_{\perp} / P$, where P is the orbital period. The small numerical enhancements to the collision frequency in this expression are (1) a factor of π (rather than 2) to account for motion of targets, i.e., each body will pass vertically through the full cross section of the swarm in somewhat less than half an orbit, (2) a factor of $2^{1/2}$ for random radial motions of the same energy magnitude as perpendicular motions, and (3) a factor of 2 for complete fragmentation occurring in collisions with cross sections greater than πa^2 (head-on) but less than $4\pi a^2$ (tangential).

Shattering of material with the tensile strength of rock occurs in collisions with specific energy greater than roughly 10^8 ergs g^{-1} (e.g., Lissauer & Griffith 1989 and references therein), corresponding to encounter speeds above 0.1 km s^{-1} . Circular orbit velocities at $r \approx 100$ AU are more than 3 km s^{-1} , so conditions for shattering encounters are met for average inclinations and eccentricities greater than 2° and 0.03 , respectively. Comets may have very low tensile strength (e.g., Asphaug & Benz 1994), so the comet-like bodies expected in the KB may be even more easily shattered.

A fragmentation power law $n(a) da = n_0 a^{-\beta} da$ was used, where a is particle radius and the power-law exponent β is 3.5 . The ($a^{-3.5}$) size spectrum reproduces itself continuously in a population of fragments from multiple collisions (e.g., Dohnanyi 1969). The effect of mutual grain collisions did not need to be treated explicitly in our calculations by virtue of properties of the $a^{-3.5}$ distribution: subfragments from further collisions and erosion fit under the same distribution, parameterized only by the total mass in the population. In equilibrium the “flow” of mass down from the largest sizes would be balanced by the loss at the smallest sizes due to radiation-pressure ejection (see below).

Expressions for the rate of PR-drag radial drift are found in Burns, Lamy, & Soter (1979) and Backman & Paresce (1993). The inward movement of grains from PR drag was assumed to end at Neptune’s orbit. PR drag would also work to circularize the motion of fragments released into eccentric orbits, so fragments were assumed to remain initially close to the heliocentric radii at which they were created. Grains smaller than a few microns released from parent bodies in near-circular orbits can be ejected by solar radiation (e.g., Burns et al. 1979) quickly compared with the PR drift times characterizing our model. For example, a 1 μm grain would move from 30 to 100 AU in a few times 10^2 yr, whereas a 2 μm grain would move inward across the same span in a few times 10^6 yr. Grains smaller than the “blowout” size were for this reason removed from the model when created. We did not consider effects of the solar wind that might act to enhance PR drag and radiation pressure ejection.

Grain temperatures were calculated using expressions from Backman & Paresce (1993) for the thermal equilibria and emitted spectra of generic grains. Absorptive efficiency was assumed to be $\varepsilon = \text{constant} = (1 - \text{Albedo})$ at visual wavelengths. Emissive efficiency was assumed to be $\varepsilon = 1$ for wavelengths smaller than the grain size a , and $\varepsilon = a/\lambda$ for $\lambda > a$. A grain with a 1 μm radius would absorb incoming solar radiation more efficiently than it emitted far-IR radiation and would have a temperature of about 100 K at $r = 30$ AU for visible albedo = 0.5 . A grain of the same composition with radius greater than 100 μm (“blackbody” grain, larger than

wavelengths of emission, therefore efficient and cool) at the same location would have a temperature of about 40 K.

Fragments of comets were assumed to be mostly water ice that should sublime if they are produced at, or drift into, regions with $T \gtrsim 100$ K (e.g., Lien 1990). Temperatures this high would be reached only by particles in the micron-size range at the inner edge of the KB. The sublimation rate for small water ice grains in a vacuum is such a powerful function of temperature that the destruction of small grains under such circumstances can be considered instantaneous. Grains that were calculated to have temperatures greater than 100 K were removed from the model.

2.2. Model Parameters

The KB was assumed to contain $0.3 M_{\oplus}$ (1.8×10^{27} g) of comets spread over heliocentric radii 30 – 100 AU with a perpendicular (“face-on”) surface number density distribution $\sigma(r) \propto r^{-\alpha}$ in which $\alpha = 2$, as in other models of the KB large-body population (e.g., Jewitt & Luu 1995). The KB was further assumed to have a “wedge” geometry, i.e., the figure of rotation of an open angle in ecliptic latitude subtended at the Sun and centered at latitude 0° , with full thickness $\Delta i = 0.3$ rad (17°). This is approximately the common inclination range observed for large KB objects and short-period comets (Jewitt & Luu 1995). The total IR surface brightness seen from Earth would be inversely proportional to Δi .

The comets themselves were assumed to be spheres with diameters of 10 km, somewhat smaller than Halley’s comet (e.g., Wilhelm 1987). Much larger objects exist in the KB, but small objects are likely to dominate the number density and collision cross-sectional area. Comets were assumed to break into spherical fragments with radii distributed as ($a^{-3.5}$) over the range 2.5 km (one-half the parent size) to 1 μm . The material density of both comets and fragments was assumed to be 0.5 g cm^{-3} , appropriate for loosely bound cometary material (Asphaug & Benz 1994; Solem 1994).

The albedo of the grains was assumed to be 0.5 . This is much higher than the value for short-period comet surfaces ($P \sim 0.04$; e.g., Jewitt 1991) but might represent unaltered interior material that would dominate the surface area exposed in a catastrophic collision. The albedo controls the relation between heliocentric radius and grain temperature: a high albedo yields a conservative lower limit to the far-IR flux predicted by the model. Albedo also linearly enhances PR drag and radiation pressure-driven ejection.

With $M_{\text{total}} = 0.3 M_{\oplus}$, $\rho = 0.5$ g cm^{-3} , $a_c = 5$ km, and radial power law $\alpha = 2$, there would be 7×10^9 comets in the entire 30 – 100 AU range, 40% of which would be between 30 and 50 AU. The equivalent surface mass density is 1×10^{-3} g cm^{-2} at 30 AU. There would be 0.03 collisions per year at $r = 30$ – 31 AU. It is important to note that the total collision rate scales as the square of the total KB mass, e.g., if the mass were increased from 0.3 to $1.0 M_{\oplus}$ then the collision rate, dust surface area, and far-IR emission would increase by a factor of 11 . If other aspects of the model are kept constant including largest fragments being one-half the parent size, then dust surface area and IR flux will scale with comet radius as ($a_c^{-1.5}$).

2.3. Model Procedures

The KB model was divided into $\Delta r = 1$ AU annuli between r_{min} and r_{max} . The collision rate was calculated for each annulus based on the formulae in § 2.1. Grain size was divided into bins of $\Delta a = 0.1$ μm . The steady state population for each spatial annulus and grain size was calculated by assuming that the sum

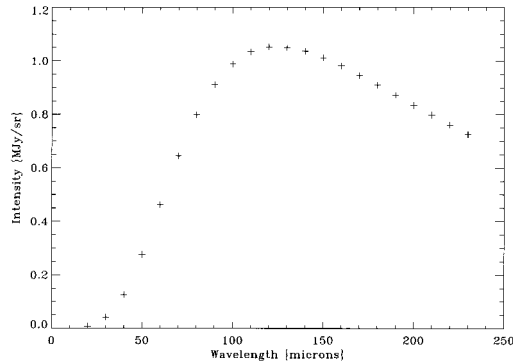


FIG. 1.—Model spectral energy distribution for the surface brightness of the entire KB dust cloud, corresponding to $0.3 M_{\oplus}$ of comets distributed over $r = 30\text{--}100$ AU with $\sigma \propto r^{-2}$ and evenly across the latitude range $\pm 8^{\circ}5$. The surface brightness would scale as the square of the total mass of KB comets.

of (1) production rate in an annulus via collisions plus (2) PR flow rate into the annulus from the next one outward, balanced (3) PR flow rate out of the annulus inward: $[N_c(r_1, r_2) f(a_1, a_2) / t_{\text{coll}}(r_1)] + [2\pi r_2 \sigma(r_1, r_2, a_1, a_2) v_{\text{PR}}(r_2)] = [2\pi r_1 \sigma(r_1, r_2, a_1, a_2) v_{\text{PR}}(r_1)]$, where $N_c(r_1, r_2)$ is the number of comets in the radial annulus, $f(a_1, a_2)$ is the number of fragments produced in a size range (a_1, a_2) per collision, and v_{PR} is the PR radial drift rate. These equations were solved for $\sigma(r_1, r_2, a_1, a_2)$, the surface number density of grains in the given annulus and grain size interval. The PR flow rates in and out of each annulus are not equal because PR drift accelerates with decreasing heliocentric radius. Calculation started with the outermost annulus, which had a boundary condition of zero flow into it from outside. The position of the innermost annulus at 30–31 AU assumes complete elimination of inbound grains encountering Neptune.

A grain with a $1 \mu\text{m}$ radius, density 0.5 g cm^{-3} , and albedo 0.5 would spiral across the $r = 30\text{--}31$ AU annulus in $\sim 10^4$ yr and would cross the entire KB model from $r = 100$ to 30 AU in $\sim 10^6$ yr. A 1 mm grain with the same composition would move 1000 times more slowly. Our numerical experiments showed that little far-IR flux was added to the total emission by grains larger than 5 mm ($5000 \mu\text{m}$), so 5 mm was the maximum size considered in the surface brightness calculation. A minor correction factor (0.95–1.00) necessary to reduce the number density in inner annuli of grains larger than about 2 mm was calculated to reflect a restricted range of source annuli for PR drift within the age of the solar system.

2.4. Results and Discussion

Figure 1 shows the surface brightness spectral energy distribution (SED) for the KB model with $M = 0.3 M_{\oplus}$, $\Delta i = 0.3$ rad. The peak flux density occurs at wavelengths near $120 \mu\text{m}$. The 60/100 μm and 100/140 μm ratios are equivalent to a color temperature of about 42 K. This is close to the temperature for “blackbody” grains at the inner edge of the model. The value of r_{min} in the model is more important in controlling the SED than the value of r_{max} ; i.e., most of the thermal emission is concentrated near r_{min} by the density and temperature gradients.

The surface brightness predicted by the model at $\lambda = 100 \mu\text{m}$ is 1.0 MJy sr^{-1} ($1.0 \times 10^{-20} \text{ W m}^{-2} \text{ Hz}^{-1} \text{ sr}^{-1}$). This equals 5%–10% of the surface brightness of inner solar system zodiacal dust on the ecliptic at $100 \mu\text{m}$ (Fig. 2; see also Wheelock et al. 1994). A cold component of the zodiacal emission stronger than this and presumably with a distinct distribution in latitude probably would have been discovered and included in models of the zodiacal cloud (e.g., Reach 1988, 1992). Thus, an upper limit of $0.3 M_{\oplus}$ for 10 km diameter

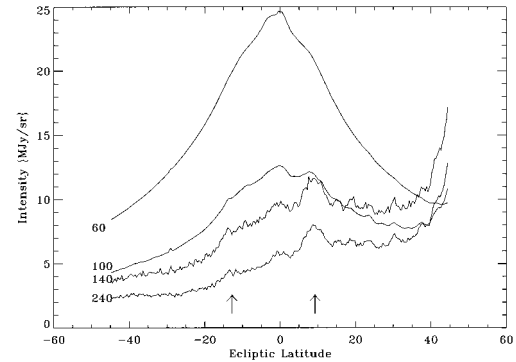


FIG. 2.—Observed far-IR surface brightness vs. ecliptic latitude at wavelengths of 60, 100, 140, and $200 \mu\text{m}$ averaged over 60° in ecliptic longitude centered at longitude 0° (COBE “Face 1,” containing the south Galactic pole). The data are from the DIRBE annual average data set. Arrows indicate a “shoulder” of emission at latitudes $+6^{\circ}$ to $+9^{\circ}$ that is much colder than the zodiacal emission centered at 0° latitude, and another, fainter “shoulder” at latitude -14° .

bodies in the zone $r = 30\text{--}100$ AU is required to yield insignificant far-IR emission from KB collision fragments relative to the observed zodiacal brightness. For comparison, Hamid, Marsden, & Whipple (1968) set an upper limit of about $1 M_{\oplus}$ on the KB mass to 50 AU from the absence of perturbations to Halley’s comet’s orbit.

The slow PR motion and enhanced radiative efficiency of large grains results in domination of the emission by grains much larger than the minimum size: 50% of the model emission is from grains larger than $a = 1.5$ mm. The total radiating dust mass in our model is about $1 \times 10^{-5} M_{\oplus}$. The bolometric luminosity of the entire KB would be about $10^{-7} L_{\odot}$. This is roughly equal to the fractional luminosity of the zodiacal dust cloud and is 10^{-2} and 10^{-4} of the fractional luminosities of the grain disks around Vega and β Pic, respectively. The far-IR emission from these stars can be approximately reproduced with KB models containing between 10 and $100 M_{\oplus}$ of comets.

Cochran et al. (1995) claim to have found approximately 50 objects with V mag $\sim +28$ in deep *HST*/WFPC2 frames. Assuming a geometric albedo of 0.04, phase function $\phi \sim 1/2$ for observations at quadrature, and minimum heliocentric distance of 30 AU, these objects have diameters of at least 20 km. The reported statistics indicate about 10^8 of them orbiting at $r = 30\text{--}50$ AU (Neptune 2:3 resonance, like Pluto) and with orbit inclinations $\lesssim 3^{\circ}3$. This represents a minimum mass of about $0.04 M_{\oplus}$ assuming material density 0.5 g cm^{-3} . However, an upper mass limit for the entire volume of our model can be derived from the *HST* observations of Cochran et al. given that (1) the observations sample 2.5 times less vertical extent, (2) the range $r = 30\text{--}50$ AU will contain 2.5 times fewer objects than the range 30–100 AU in an r^{-2} surface density distribution, and (3) there would be 4 times fewer detected objects with $d = 20$ km than in the model $d = 10$ km population if the large-body size distribution follows (d^{-2}) (Jewitt & Luu 1995). Combining these factors, it is possible that the objects reported by Cochran et al. represent a subset of as much as $1 M_{\oplus}$ of comets within the volume of our model KB. Thus, an upper limit to the KB comet population derived here from dust emission limits is significantly lower than an upper limit estimated from *HST* observations.

The model predicts 0.3 comet collisions per year in the entire $r = 30\text{--}100$ AU range, mostly in the inner regions. A lower limit to the timescale for dispersal and disappearance of a cloud of collision debris can be estimated by assuming (1) the

fastest fragments move relative to the center of mass at the parent body collision speed and (2) a discrete “knot” of debris from an impact becomes indistinguishable when its surface brightness decreases to $\leq 1/10$ of the uniform KB dust emission. This time scale is only 1/4 year at $r = 30$ AU. The model therefore predicts a chance of only about 1/10 for observing a collision debris cloud in the KB at any one time.

Duncan, Levison, & Budd (referenced in Weissman 1995) have shown that the e -folding time for the comet population at distances $r \lesssim 45$ AU due to planetary perturbations is roughly the age of the solar system. An alternate model was computed in which the inner edge of the comet population was set at 45 AU instead of 30 AU but with inward PR drift of grains continuing to Neptune. This model had virtually the same far-IR temperature of 40 K but about one-half the brightness of the original model.

3. SEARCH FOR COLD SOLAR SYSTEM DUST IN COBE DIRBE DATA

Figure 2 shows a plot of surface brightness versus ecliptic latitude at several wavelengths from the COBE DIRBE (Silverberg et al. 1993) annual average data set. The plot represents an average across 60° in longitude centered on longitude 0° . Emission from zodiacal dust peaking at latitude 0° is obvious. There is a band of emission at latitudes $+6^\circ$ to $+9^\circ$ which appears as a “shoulder” of emission that is cold relative to zodiacal dust. A similar feature with lower contrast at a latitude of about -14° may be discerned in Figure 2. There is also a faint band near ecliptic coordinates (180° , -9°) (not pictured). These segments of the ecliptic were chosen for examination because they are farthest from the Galactic plane.

Most of the cold excess emission appearing in Figure 2 comes from a few bright, irregular knots with typical diameters of a few degrees (3–10 DIRBE pixels). Their color temperatures are in the range of 20–30 K. Many of these knots were cataloged as “100 μm only” cirrus sources by Paley et al. (1991) or are in the IRAS Small Scale Structure Catalog (1988). The knots have IRAS catalog positions (epoch 1983.5) within 0–3 pixels (0° – 1°) of the COBE peak brightness positions (epoch 1990.5), i.e., they have no significant secular motion. Within the limits of fairly noisy (1 week integration) data, these knots also show no 6 month parallax larger than about 0.6 (2 COBE pixels), corresponding to $r > 200$ AU.

Although the orientation of these bands approximately parallel to the ecliptic and the hint of double-banded structure (cf., e.g., Sykes 1988) is intriguing, it is unlikely that the bands are solar system material if the knots within them are not. Thus, their average surface brightness can be used to estimate an upper limit on cold excess relative to zodiacal emission in restricted latitudes near the ecliptic. These limits are approxi-

mately 0.3, 1.0, 2.5, and 2.0 MJy sr^{-1} at 60, 100, 140, and 240 μm , respectively, for features extending a few degrees in latitude.

4. SUMMARY

Far-IR emission from a model KB grain population would have a peak intensity of 1.1 MJy sr^{-1} at 120 μm and a color temperature of 42 K. The model involves grains produced by collisions of 0.3 M_\oplus of 10 km diameter comets distributed as r^{-2} from 30 to 100 AU over a latitude range of $\Delta i = \pm 8.5^\circ$. The model emission corresponds to an approximate observational upper limit for cold emission spread over that latitude range which is set by the brightness of the foreground zodiacal emission. Model far-IR intensity scales with total KB mass as M^2 , with characteristic comet radius as $a_c^{-1.5}$ and with KB thickness as $(\Delta i)^{-1}$. The upper limit to the KB comet population derived here from lack of dust emission is significantly lower than limits of about 1 M_\oplus for the same volume estimated from both HST observations and dynamical calculations.

The model KB dust fractional bolometric luminosity ($L_{\text{dust}}/L_{\text{star}}$) has about 10^{-2} and 10^{-4} of the values for the grain disks around Vega and β Pic, respectively. The far-IR emission from these two stars’ circumstellar disks can be approximately reproduced by KB models containing, respectively, 3 and 30 M_\oplus of comets. Further work modeling the evolution of KB-like comet and dust populations from stellar ages of 10^7 – 10^8 yr to the age of the solar system will be reported in a future paper.

Cold nonuniform bands with latitude widths of a few degrees near the ecliptic discernible in COBE DIRBE data have brightnesses averaged over 60° longitude of ≈ 1 –2 MJy sr^{-1} at 100–240 μm . These probably do not represent solar system material, but future observations may help distinguish foreground from galactic emission.

The authors are grateful for help received from Tom Kelsall, Jeff Newmark, Dave Leisawitz, and Gayle Rawleigh in the COBE group at NASA/Goddard. The COBE data sets were developed by the NASA/Goddard Space Flight Center under the guidance of the COBE Science Working Group and were provided by the NSSDC. We thank Michelle Creech-Eakman, Dale Cruikshank, Roc Cutri, Richard Greenberg, and Jane Luu for helpful discussions and comments. This research was made possible in part by NASA grant NAGW-3680 (ISO US Key Projects) to the University of Denver and a grant from the 1994 Hackman Summer Undergraduate Research Program at Franklin and Marshall College. A preliminary version of this model was presented as a poster at the 1995 January AAS meeting (Dasgupta & Backman 1995). A preprint of a study with similar intent to ours (Stern 1995) was received as we prepared this Letter.

REFERENCES

- Asphaug, E., & Benz, W. 1994, *Nature*, 370, 120
 Aumann, H. H., & Good, J. C. 1990, *ApJ*, 350, 408
 Backman, D. E., & Paresce, F. 1993, in *Protostars and Planets III*, ed. E. H. Levy & J. I. Lunine (Tucson: Univ. of Arizona Press), 1253
 Burns, J., Lamy, P. L., & Soter, S. 1979, *Icarus*, 40, 1
 Cochran, A., Levison, H. F., Stern, S. A., & Duncan, M. J. 1995, *ApJ*, in press
 Dasgupta, A., & Backman, D. E. 1995, *BAAS*, 26, 1376
 Dohnanyi, J. 1969, *J. Geophys. Res.*, 74, 2531
 Hamid, S. E., Marsden, B., & Whipple, F. 1968, *AJ*, 73, 727
 Harper, D. A., Loewenstein, R. F., & Davidson, J. A. 1984, *ApJ*, 285, 808
 IRAS Small Scale Structure Catalog 1988, prepared by G. Helou & D. Walker (Washington, DC: GPO)
 Jewitt, D. C. 1991, in *Comets in the Post-Halley Era*, ed. R. Newburn, M. Neugebauer, & J. Rahe (Dordrecht: Kluwer), 19
 Jewitt, D. C., & Luu, J. X. 1995, *AJ*, 109, 1867
 Lien, D. J. 1990, *ApJ*, 355, 680
 Lissauer, J. J., & Griffith, C. A. 1989, *ApJ*, 340, 468
 Paley, E. S., Low, F. J., McGraw, J. T., Cutri, R. M., & Rix, H.-W. 1991, *ApJ*, 376, 335
 Reach, W. T. 1988, *ApJ*, 335, 468
 ———. 1992, *ApJ*, 392, 289
 Silverberg, R. F., Hauser, M. G., Boggess, N. W., Kelsall, T. J., Moseley, S. H., & Murdock, T. L. 1993, *Proc. SPIE* 2019, 180
 Solem, J. C. 1994, *Nature*, 370, 349
 Stern, S. A. 1995, *A&A*, submitted
 Sykes, M. V. 1988, *ApJ*, 334, L55
 Weissman, P. R. 1984, *Science*, 224, 987
 ———. 1995, *ARA&A*, in press
 Wheelock, S. L. 1994, *IRAS Sky Survey Atlas Explanatory Supplement* (JPL Pub. 94-11) (Pasadena: JPL)
 Wilhelm, K. 1987, *Nature*, 327, 27